

Lessons from Simulation Regarding the Control of Synthetic Self-Assembly

Jack F. Douglas and Kevin Van Workum[†]

National Institute of Standards and Technology, Polymers Division, Gaithersburg, Maryland 20899, [†] Present address: US Naval Academy, Annapolis, MD 20142

ABSTRACT

We investigate the role of particle potential symmetry on self-assembly by Monte Carlo simulation with the particular view towards synthetically creating structures of prescribed form and function. First, we establish a general tendency for the rotational potential symmetries of the particles to be locally preserved upon self-assembly. Specifically, we find that a dipolar particle potential, having a continuous rotational symmetry about the dipolar axis, gives rise to chain formation, while particles with multipolar potentials (e.g., square quadrupole) having discrete rotational symmetries led to the self-assembly of *random surface* polymers preserving the rotational symmetries of the particles within these sheet structures. Surprisingly, these changes in self-assembly geometry with the particle potential symmetry are also accompanied by significant changes in the thermodynamic character and in the kinetics of the self-assembly process. Linear chain growth involves a continuous chain growth process in which the chains break and reform readily, while the growth of the two-dimensional polymers only occurs after an 'initiation' or 'nucleation' time that fluctuates from run to run. We show that the introduction of artificial seeds provides an effective method for controlling the structure and growth kinetics of sheet-like polymers. The significance of these distinct modes of polymerization on the functional character of self-assembly growth is illustrated by constructing an artificial centrosome structure derived from particles having continuous and discrete rotational potential symmetries.

INTRODUCTION

Molecular self-assembly at equilibrium is central to the formation of numerous biological structures [1-3] and the emulation of this process through the creation of synthetic counterparts [4-9] offers great promise for nanofabrication [10-15]. The central problems in this field are an understanding of how the symmetry of interacting particles encodes information about the geometrical structure of the self-assembled structure and the nature of the thermodynamic transitions governing this type of organization.

A first attempt at establishing principles for molecular self-assembly was made by Crick and Watson in the case of the protein shells of viruses. [16] They argued that viral shell structures assembled from *equivalent protein particles* must have the form of hollow tubes (helical in general) or closed shell structures belonging to the family of Platonic polyhedra (cube, tetrahedron, octahedron, dodecahedron, icosahedron) where each particle has an *equivalent local environment* with its neighbors. The equivalence of the local environment requires that a permutation of particles within these structures preserves their local interactions within the organized structure so that Crick and Watson's arguments amount to the hypothesis that the local particle potentials within the self-assembled structures are *invariant under particle permutation*, P . Crick and

Watson's claims [16] were soon supported by electron microscopy and x-ray diffraction measurements indicating that polio virus had an icosahedral viral shell ('capsid'), [1,17] but Caspar and Klug [3] later amended these symmetry arguments to allow for the local inequivalence ('quasi-equivalence') of molecular environments that were found in subsequent investigations of viral capsid structure. [Molecular 'switches' involving changes of molecular conformation of the particles (proteins) involved in self-assembly are normally invoked to rationalize these deviations from 'equivalence' that allow 'spherical' virus capsids to become indefinitely large.] Caspar and Klug further argued that the general tendency to minimize the defect energy of the viral capsid selects out a *unique family* of icosahedral symmetry structures in which hexagonal units are inserted between the pentagonal units at the vertices of an icosahedron, a family of shell structures that they term 'icosadeltahedra'. Most spherical viruses have been found to conform to this type of organization. [1, 17]

The symmetry arguments of Crick and Watson [16] do not make any prescription about the particular geometrical form of the self-assembled structure in relation to the symmetry properties of the sub-particles. Self-assembling systems are often characterized by strong directional interactions (e.g., dipolar) with well-defined rotational symmetries [18] and, by extending the intuitive reasoning of Crick and Watson, we anticipate that these rotational symmetries tend to be *locally* preserved in the self-assembled structure. In the next section, we explore this hypothesis with model multipole potentials.

MULTIPOLE INTERACTION MODELS OF SELF-ASSEMBLY

Monte Carlo simulation methods

At gas phase densities, the simulation of strongly associating systems can present challenges for traditional simulation techniques. The strong binding energies between associated particles and large distances between non-associated particles can make sampling of important regions of configuration-space difficult [19]. The time required for particles to undergo an association/disassociation transition can be very long compared to typical molecular dynamics simulation times. There are Monte Carlo algorithms that can overcome these difficulties, however. In this work, we use the Aggregate Bias Monte Carlo algorithm [20] to improve the sampling of relevant regions of configuration space and enhance the sampling of clusters. At the heart of this algorithm is an intra-box swap move that is targeted at sampling the formation or destruction of clusters. We also implement the simple translational and rotational moves to explore nearby regions of phase space. A detailed discussion of this method is given in our previous paper devoted to the Stockmayer fluid [18], which is defined in the next section.

Symmetries of multipole particle potentials and the 'equivalence principle'

Stimulated by the philosophical approaches of Crick and Watson [16] and Casper and Klug [3], we introduce a family of minimal ('schematic') models that can serve as a testing ground for understanding principles of self-assembly. Our approach builds on our recent systematic investigation of the Stockmayer fluid (SF) involving a fluid having a competition between dipolar (See Fig. 1a) and van der Waals interactions and which is established to exhibit the formation of equilibrium linear polymer chains upon cooling.

[18] This is a natural starting point for investigating protein self-organization since proteins are often characterized by large dipolar (e.g., the dipole moments of tubulin, collagen and sickle cell hemoglobin(S) dimers are 1410 D, 1150 D and 545 D, respectively [22]) or directional hydrogen bonding interactions and it seems likely these highly directional interactions must be part of any explanation of molecular self-assembly of proteins in solution ($1 \text{ D} = 3.336 \times 10^{-30} \text{ Coulomb} \cdot \text{m}$). The dipolar potential has a $C_{\infty v}$ point group symmetry which is a *continuous rotational symmetry*. Next, we consider a *point quadrupole* generalization of the SF [23] that approximately models two side-by-side and head-to-tail dipoles or four charged particles (two plus and two minus charged particles; See Fig. 1) in a square ring. The special case of the square quadrupole potential ($\theta = \pi / 2$) evidently exhibits a discrete (D_{2h}) point group symmetry. We also consider a triangular configuration of SF particles that have a head-to-tail configuration (See Fig. 1c), which is characterized by a C_3 discrete rotational symmetry. If we formally extend the reasoning of Crick and Watson to require that these potentials preserve their local symmetries in the organized structure, then we should expect chain-like structures in the continuous rotational potential case of the SF (known to be the case) and *two-dimensional polymers* to form for the particle potentials having a discrete symmetry rotational potential (In particular, the potentials in Figs. 1b and 1c should lead to sheet-like polymers having rectangular and hexagonal symmetries, respectively.). Notably, it is the *symmetries* of the potentials that are primarily important in our considerations below and similar patterns of self-assembly can be expected for other potentials (hydrogen bonding, π - π interactions and localized hydrophobic interactions, strong-segregation block copolymers in solution, grafted polymer chains on nano-particles having attachment points of prescribed symmetry, etc.) exhibiting strong directional interactions with the same point group symmetries.

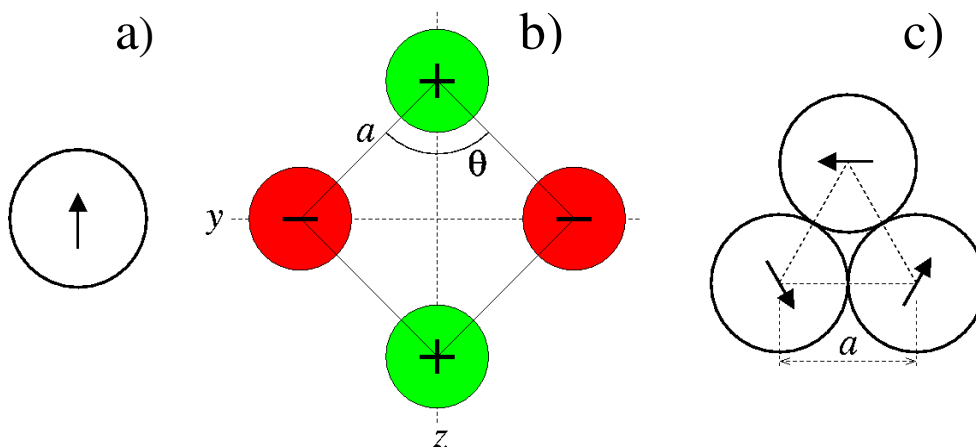


Figure 1. Multipole potentials of particles with directional interactions. a) dipole, b) quadrupole, c) 'hexapole'.

Stockmayer fluid

First, we briefly recall some basic aspects of self-assembly in the SF. [18] Two particles in the SF interact via a Lennard-Jones (LJ) potential and an additional point dipole potential placed the center of each particle (Fig. 1a). The dipolar contribution to the potential is given by,

$$u_{\text{dipole}} = (\boldsymbol{\mu}_i \cdot \boldsymbol{\mu}_j) / r_{ij}^3 - 3 (\boldsymbol{\mu}_i \cdot \mathbf{r}_{ij}) (\boldsymbol{\mu}_j \cdot \mathbf{r}_{ij}) / r_{ij}^5 \quad (1)$$

where $\boldsymbol{\mu}_i$ is the dipole moment of particle i and $\mathbf{r}_{ij} = \mathbf{r}_i - \mathbf{r}_j$ is the interparticle separation and the LJ contribution to the potential ($u_{\text{SF}} \equiv u_{\text{LJ}} + u_{\text{dipole}}$) has the familiar form,

$$u_{\text{LJ}} = 4 \varepsilon [(\sigma / r_{ij})^{12} - (\sigma / r_{ij})^6], \quad (2)$$

where the van der Waals (vdW) interaction energy strength ε controls the magnitude of the potential minimum, and σ is a measure of particle ‘size’. It is conventional to define a dimensionless measure of the dipole interaction energy relative to the vdW energy, $(\mu^*)^2 = \mu^2 / \varepsilon_D \sigma^3 \varepsilon$ where ε_D is the dielectric constant of the fluid background medium. All concentrations ρ are number densities and T is normalized by ε / k_B where k_B is Boltzmann’s constant.

In a previous investigation [18], we mapped out the thermodynamic transition lines for the SF as a function of ρ and T in the low density regime. Upon cooling, there is a self-assembly (‘polymerization’) transition where dipolar particle chains form and disintegrate in a state of *dynamic equilibrium* (Fig. 2). The location of the transition curves defining this transformation are found to be well-described by the theory of equilibrium polymerization [18, 21], where the sticking energy (enthalpy of association [21]) is uniquely fixed by the minimum in the intermolecular potential between two SF particles [18]. At low temperatures, the long-range dipolar interaction causes the chains

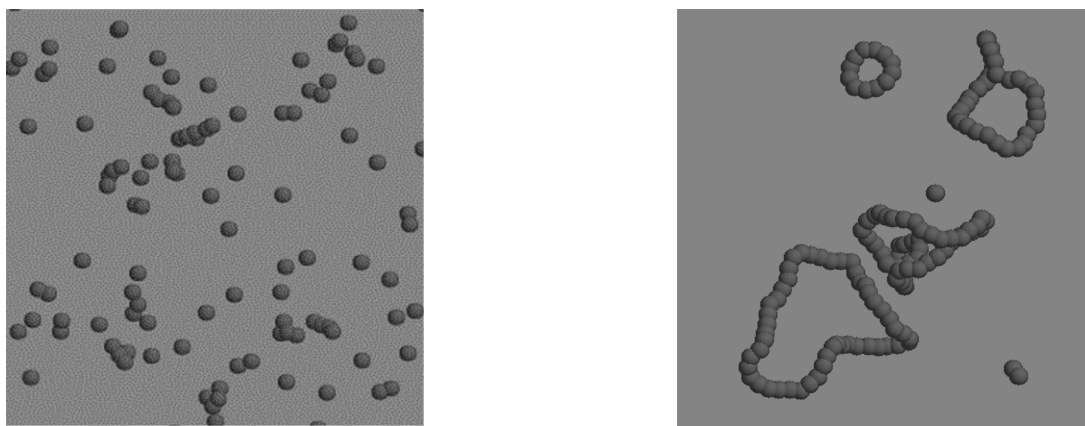


Figure 2. Polymerization transition in the Stockmayer fluid (SF) upon cooling [18]; a) Left; $T = 10.0$, b) Right; $T = 7.80$. The number density ρ is constant, $\rho = 0.001$.

to form ring structures that minimize their energy. [18] This *topological transition* occurs despite the entropic energetic cost of confining the free ends of the chains into rings. Figure 2 shows the change in organization as T is lowered through the transition temperature ($T_\Phi = 9.5$ at this concentration [18]).

The growth of the average (equilibrium) length of the chains upon cooling and their shrinking upon heating are quite reversible in the SF; no nucleation seems to be required for this growth process. Fluctuations in thermodynamic variables [average energy E , extent of polymerization Φ (fraction of particles in assembled state), average chain length L , etc.] become large and long-lived near the polymerization transition temperature, T_Φ , and the specific heat C_p shows a maximum near T_Φ , reflecting these fluctuations. The smooth and reversible nature of the polymerization in the SF is completely altered by changing to potentials having discrete rotational symmetries, however. [23]

Quadrupole / van der Waals fluid

The inclusion of a point quadrupole interaction (Fig. 1b), superimposed on the van der Waals interaction, is a direct formal generalization of the SF. The LJ component of the potential is the same as in Eq. (2) and a detailed definition of the quadrupole interaction is given in ref. [23]. As mentioned earlier, we can think of this potential here in terms the approximate four charge representation shown in Fig. 1b. Similar to the SF, we introduce a dimensionless quadrupole interaction strength relative to the van der Waals interaction as, $Q^* = Q / (4 \pi \epsilon_D \sigma^5 \epsilon)^{1/2}$ where $Q = 4a^2q$ is the ‘quadrupole strength parameter’, defined as in terms of the charge q and the charge separation a (See Fig. 1b).

We see from Fig. 2 that the continuous rotational symmetry of the dipolar particles about their symmetry axis is approximately preserved in the organized structure (nearby particles can create perturbations in the potential so the symmetry preservation is only approximate). The rotational freedom of the resulting particle chains causes the assembled structures to be ‘floppy’ and one-dimensional by nature, at least when the attractive van der Waals interactions are not strong enough to induce chain collapse. [24] The discrete rotational symmetry of the Quadrupole/van der Waals (Quad/vdW) fluid (Fig. 1b) that generalizes the SF indeed gives rise to structures exhibiting an approximately two-fold local symmetry within the assembled sheet-like polymers. In Fig. 3, we show a representative ‘random surface’ polymer that spontaneously assembled in the Quad/vdW fluid at low temperatures. We observe that the ‘dipoles’ comprising the quadrupole exhibit a strong tendency to form local closed loops within the sheet (See Fig. 3), reminiscent of the SF. These two-dimensional or ‘random surface’ polymers tend to roll up in one direction to form ‘nanotubes’ (See Fig. 3) [23], providing a two-dimensional polymer analog of ring formation in the SF. Thus, the organization of both the SF and the Quad/vdW fluids are both driven by directional interactions and the local symmetries in the particle potential are approximately preserved in the organized structure, as hypothesized above. A similar pattern of behavior is found for the triangular (‘hexapole’) configuration of dipolar particles shown in Fig. 1c, which has a three-fold rotational symmetry. In this case, we find the formation of both open hexagonal random surfaces [23], as well as closed icosahedral shells. [23] The formation of closed icosahedra is evidently another generalization of SF ring formation to the two-

dimensional polymers of the hexapole model where the sheets effectively fold up along two orthogonal directions of the sheet to form closed shells. This mode of shell formation conforms to the ‘equivalence’ arguments of Crick and Watson. [16]

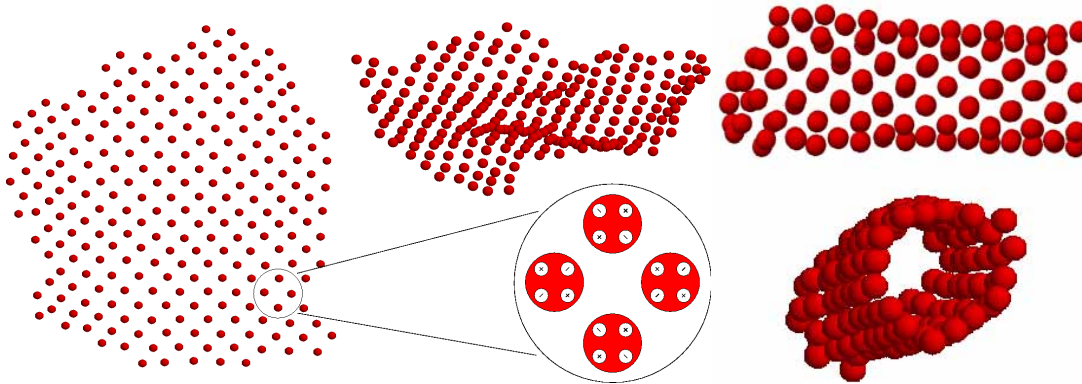


Figure 3. Random surface and ‘nanotubes’ formed by square Quad/van der Waals fluid. Left image indicates a top view of a representative random surface polymer ($T = 1.35$, $Q^* = 1.0$, $\rho = 0.001$) and a profile view is shown in top middle. Inset shows local ‘charge configuration’ within the ‘sheet’. Right images shows side (upper image) and profile view (lower image) of self-assembled ‘nanotubes’ ($T = 1.7$, $Q^* = 2.0$, $\rho = 0.001$).

We note that if we change the angle θ of the quadrupole potential from $\pi/2$ to $\theta = \pi/4$ (See Fig. 1b), it becomes difficult for the particles to form into random surfaces as in Fig. 3. [23] Evidently, the symmetry properties of the particle potential must be consistent with allowable surface tiling symmetries for sheet formation to occur. Previous simulations for particles having a linear quadrupole interactions along with an anisotropic hard-core interaction (model of exfoliated clay particles) led to the formation of ‘branched equilibrium polymers,’ [25] which can be thought of as random surfaces having a disordered topological structure. [23] Branched equilibrium polymers were also found for our simulations for $\theta = \pi/4$. [23]

CONTROLLING SELF-ASSEMBLY WITH SEEDS

Inserting seeds of specific symmetry provides an important source of control over the geometry of self-assembly and the kinetics of growth. Seeding also provide a way of imposing growth symmetries that are not shared by the potential of the assembling particles. *Templating* [26] occurs in many biological systems to regulate self-assembly into unique or nearly unique growth forms and we can expect this process to serve as a powerful tool in controlling synthetic nanofabrication. Unwanted templating can lead to disease and the misdirection of synthetic self-assembly into unwanted growth forms.

Figure 4 illustrates the growth of a hollow cylinder (nucleated from a seed having the form of a ring of hexagons). This heterogeneous nucleation process leads to the propagating growth of a cylinder with a hexagonal local symmetry (Hex/vdW model; See Fig. 1c), a structure that does not seem to readily form in the absence of a seed. Moreover, by making the seed anisotropic (by making particles on one side of the hexagon ring simple vdW particles), we find that we can obtain *directional growth along*

one direction. [23] Such ‘polarized growth’ growth is characteristic of many biological self-assembly processes, such as microtubule growth emanating from the centrosome in the course of mitosis [27].

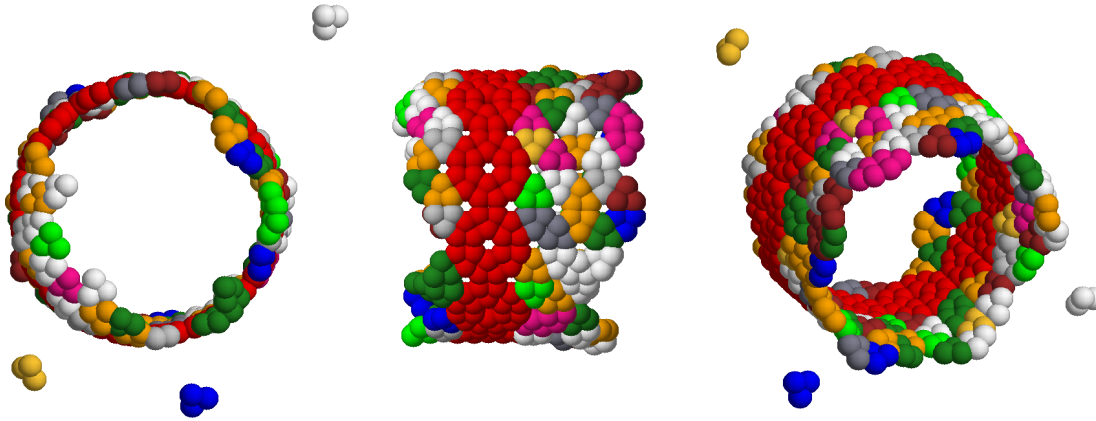


Figure 4. Seeded nanotube formation in the Hex/vdW fluid. Images show from left to right: end-on, side-view and profile views. Conditions: $T = 7.85$, $\mu^* = 6.0$, $\rho = 0.001$.

The introduction of an artificial seed has a dramatic influence on the evolution of the self-assembly process. The growth kinetics without the seed exhibits intense fluctuations in the time at which for which assembly growth initiates. [23] By eliminating the requirement for homogeneous nucleation of a seed structure, we find that the growth curves describing the self-assembly process become much more reproducible, having a form reasonably similar to the SF. Seeding thus generally reduces the average time required for the initiation or ‘nucleation’ of growth assembly and serves to regulate the ultimate assembly geometry by encoding the symmetry characteristics of the seed with those of the assembling particles into self-assembling structures.

An artificial centrosome: one-dimensional versus two-dimensional polymers

We have seen that an apparently modest change in the character of the particle potential (dipole to quadrupole or hexapole) can give rise to dramatic changes in the assembly structure and growth kinetics. It is interesting to consider the implications of this change in interaction potential type on the functional character of the assembly process. A full treatment of this problem will require molecular dynamics simulations, but we can obtain some qualitative insights into this question by Monte Carlo simulation.

The cytoplasm is conspicuously composed of two primary self-assembling proteins—actin and tubulin. The first cytoskeleton protein, actin, can form reversible polymers as in the case of the dipolar fluid, while tubulin polymerizes as a sheet-like polymer in a highly directional fashion. This directional growth has been studied *in vitro* by introducing artificial seeds (synthetic analogs of ‘centrosomes’). [28]

Given the quasi-two dimensional nature of the experiments, we restrict ourselves to a plane. Our seed (See Fig. 5) is a hexagon of hexapole particles as in Fig. 4 where the

dipoles point outward radially (μ^* for the centromere-inspired seed was taken to equal 12.0, while μ^* for the other particles equals 6.0.). There were 32 particles confined to within a circle of diameter 25 ($\rho = 0.0652$) where the dipoles were allowed to orient in any direction in three-dimensional space and $T = 12.0$, which was sufficiently low T to

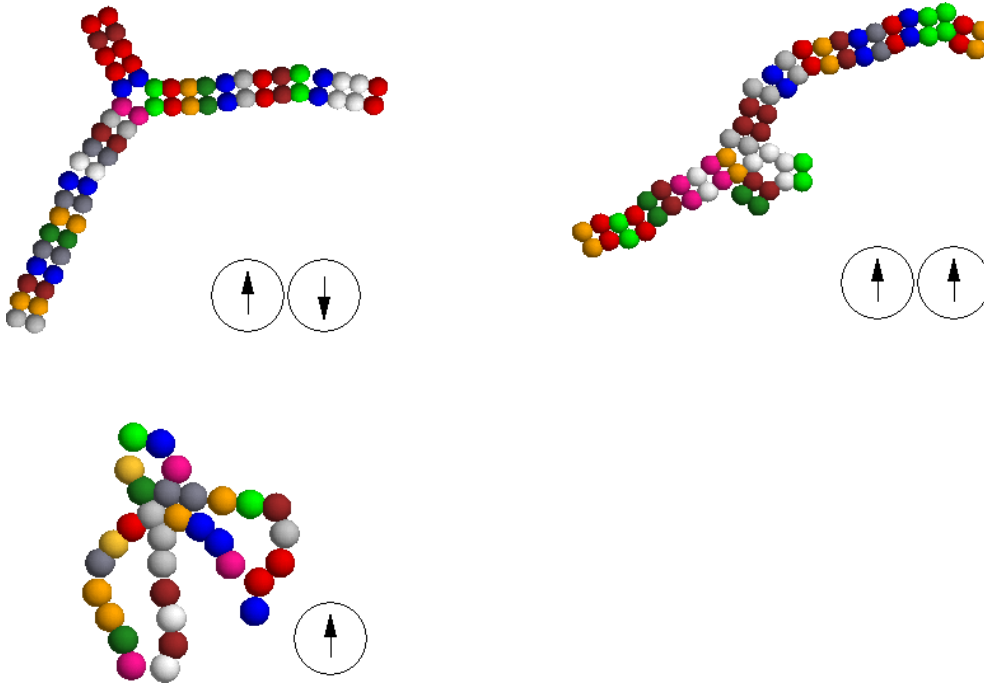


Figure 5. Polymerization from artificial centrosome in two-dimensions: parallel, anti-parallel, and single dipole particles. Particles are free to rotate their dipoles out of plane.

induce polymerization in this quasi-two-dimensional fluid. (It should be appreciated that this simulation involves a rapid deep quench so that the resulting structures are not at equilibrium.) We compare three classes of particles: ordinary hard sphere with a point dipole at their center and pairs of such dipoles in a parallel and anti-parallel orientation. The dipolar particles, with their continuous local rotational symmetry, grew into chains as in the SF and these structures readily grew from an artificial seed, as shown in Fig. 5. Seeding of a sort is evidently possible for dipolar particles. The chains that formed had the property of breaking within their interiors while they were growing and these dynamic structures then recombined with other polymer arms or the initial arm of the growing star polymer. There was also tendency for the rings to close into loops as the chains became long so that multi-loop structures arise. It is clear that the growth of such structures cannot exert a coherent interaction on its surroundings, as required for effective centromere growth. On the other hand, the multipole analogs of the dipolar sphere model exhibit a rather different type of growth process. These structures likewise ‘nucleate’ off a core seed (artificial ‘centrosome’), but the growth becomes *highly directed* from the ends of the growing fiber-like structures composed of discrete rotational symmetry particles. It is easy to imagine that growing structures of this kind could exhibit a force on their environment. Such a growth process could also be the source of active molecular

transport. It would appear that the self-assembly processes illustrated in Fig. 5 could perform complementary functional tasks. Such differences of growth dynamics are perhaps a contributing factor to the origin of the multiple types of assembling proteins (actin, tubulin, intermediate filaments) found in living cells.

Conclusions

We have sought to understand how the symmetry properties of the interaction potential of model fluids influence the geometrical structure of self-assembly. We find that there is a general tendency for the point group symmetries of the particle potentials to be preserved under self-assembly and we obtain insight into the origin of chain-like and random surface structures with local rectangular and hexagonal symmetries based on simple multipole potential models. Biological molecules characteristically exhibit large Coulombic, dipolar and multipole interactions (or interactions exhibiting the same point group symmetries) so that this class of potentials is promising for investigating broad trends in biological and synthetic self-assembly. We also show that polymorphic character of the self-assembly process in the case of formation of two-dimensional polymers can be regulated with artificial seeds of prescribed symmetry. Seeding also serves to regulate the kinetics of self-assembly, reducing the fluctuations in the nucleation time. The differing nature of the self-assembly process in the case of continuous and discrete rotational symmetry particles is shown to have functional implications through our example of an ‘artificial centrosome’. Future work should consider a combination of multipole (dipole, quadrupole, octapole) interactions since these interactions are simultaneously present in real proteins. Transitions between self-assembled structures having different symmetry and topological characteristics can be expected to result from changing the relative strengths of these directional interactions. A transition of this kind might explain the transition of microtubules from a nanotube to a ring configuration under exposure to certain drugs or viral infection. [29]

ACKNOWLEDGEMENT

KVW would like to thank the National Research Council and NIST for support.

REFERENCES

1. A. Klug, *Proc. Roy. Soc. A* **348**, 167 (1994).
2. F. Oosawa and S. Asakura, *Thermodynamics of the Polymerization of Protein* (Academic Press, New York, 1975).
3. D. L. D. Caspar and A. Klug, *Cold Spring Harbor Symp. Quant. Biol.* **27**, 1 (1962); See also: D.L. D. Caspar, *Biophys. J.* **32**, 103 (1980); L. Makowski, *Biophys. J.* **74**, 534 (1998); A. Klug, *Nature* **303**, 378 (1983); J. J. Johnson and J. A. Spier, *J. Mol. Biol.* **269**, 665 (1997); M. S. Chapman, *Biophys. J.* **74**, 639 (1998).
4. D. Philp and J. F. Stoddart, *Angew. Chem.-Int. Edit. Engl.* **35**, 1155 (1996).
5. J. S. Moore, *Current Opinion Coll. Int. Sci.* **4**, 108 (1999).
6. J. M. Lehn, *Supramolecular Chemistry* (VCH, Weinheim, 1995).

7. A. P. Alivisatos, K. P. Johnsson, X. G. Peng, T. E. Wilson, C. J. Loweth, M. P. Bruchez and P. G. Schultz, *Nature* **382**, 609 (1996).
8. S. A. Jeneke and X. L. Chen, *Science* **283**, 372 (1999).
9. L. Brunsveld, B. J. B. Folmer, E. W. Meijer and R. P. Sijbesma, *Chem. Rev.* **101**, 4071 (2001).
10. B. J. de Gans, S. Wiegand, E. R. Zubarev, and S. I. Stupp., *J. Phys. Chem. B* **106**, 9730 (2002).
11. S. I. Stupp, S. Son, H. C. Lin, and L. S. Li, *Science* **259**, 59 (1993); S. I. Stupp, V. LeBonheur, K. Walker, L. S. Li, K. E. Huggins, M. Keser, and A. Amstutz, *Science* **276**, 384 (1997).
12. C. A. Mirkin, R. L. Letsinger, R. C. Mucic, and J. J. Storhoff, *Nature* **382**, 607 (1996).
13. J. Schnur, *Science* **262**, 1669 (1993).
14. M. R. Ghadiri, J. R. Granja, R. A. Milligan, D. E. McRee and N. Khazanovich, *Nature* **366**, 324 (1993). See also: J. –H. Furhop and W. Helfrich, *Chem. Rev.* **93**, 1565 (1993).
15. D.S. Lawrence, T. Jiang, M. Levelt, *Chem. Rev.* **95**, 2229 (1995).
16. F. H. C. Crick and J. D. Watson, *Nature* **177**, 473 (1956).
17. J. T. Finch and A. Klug, *Nature* **183**, 1709 (1959); See also: J. B. Bancroft, *Advances in Virus Research* (Academic, New York, 1970); M. G. Rossmann and J. E. Johnson, *Ann. Rev. Biochem.* **58**, 533 (1989).
18. K. Van Workum and J. F. Douglas, *Phys. Rev. E* **71**, 031502 (2004); J. Staumbaugh, K. Van Workum and J. F. Douglas and W. Losert, *Phys. Rev. E* **72**, 031301 (2005).
19. J. C. Shelley, G. N. Patey, D. Levesque, and J. J. Weis, *Phys. Rev. E* **59**, 3065 (1999).
20. B. Chen and J. I. Siepmann, *J. Phys. Chem. B* **105**, 11275 (2001).
21. J. Dudowicz, K. F. Freed, and J. F. Douglas, *J. Chem. Phys.* **112**, 1002 (2000); *J. Chem. Phys.* **113**, 434 (2000); *J. Chem. Phys.* **119**, 12645 (2003).
22. J. Staumbaugh, PhD Thesis, University of Maryland (College Park), 2004. The raw data from which the dipole moments were calculated was obtained from the protein databank.
23. K. Van Workum and J. F. Douglas, *Mackromol. Symp.* **227**, 1 (2005); *Phys. Rev. E* (submitted).
24. P. R. ten Wolde, D. W. Oxtoby and D. Frenkel, *Phys. Rev. Lett.* **81**, 3695 (1988).
25. M. Dijkstra, J. P. Hansen, and P. A. Madden, *Phys. Rev. Lett.* **75**, 2236 (1995); *Phys. Rev. E* **55**, 3044 (1997).
26. Z. Cao and F. A. Ferrone, *Biophys. J.* **72**, 343 (1997); J. King and S. Casjens, *Nature* **251**, 112 (1974); A. Klug, *Angew. Chem : Int. Edn.* **22**, 565 (1983).
27. D. K. Fygenson, E. Braun and A. Libchaber, *Phys. Rev. E* **50**, 1579 (1994); H. Flyvbjerg, T. E. Holy and S. Leibler, *Phys. Rev. E* **54**, 5538 (1996).
28. T. E. Holy, M. Dogterom, B. Yurke and S. Leibler, *Proc. Nat. Acad. Sci.* **94**, 6228 (1997); F. J. Nédélec et al., *Nature*, **389**, 305 (1997); V. Rodionov, E. Nadezhkina, G. Borisy, *Proc. Nat. Acad. Sci.* **96**, 115 (1999).
29. N. R. Watts et al., *J. Cell Biology* **150**, 349 (2000).